

Analysis of Observed Accelerograms to Separate Source Propagation Path and Local Site Effects

Masaru TAI, Yoshinori IWASAKI
Osaka Soil Test Laboratory, Osaka, Japan

Soji YOSHIKAWA
Association of Disaster Prevention Research, Kyoto, Japan

Kojiro IRIKURA
Kyoto Univ., Uji, Japan

Toru NAGANO, Masahiko OZAKI
The Kansai Electric Power Company Inc., Osaka, Japan

ABSTRACT

In this paper, we try to evaluate source effects, propagation path effects in connection with the geometrical attenuation and anelasticity (Q-value) as well as local site effects in frequency domain from S-wave of accelerograms observed in the rock. If seismic records and these spectra are obtained at several sites by different earthquakes, we can construct the simultaneous logarithmic equations with the unknown quantities such as source spectra, Qs-value and local site amplification effects. To solve these equations, we used linear inversion method setting up the criterion that local site effects have a factor of more than 1.0. This method is examined by using two data sets: one is obtained from the earthquakes M=5.7-7.0 at four stations (SZJ, TTY, HMY and CHS) and the other is obtained from the earthquakes M=5.6-6.6 at three stations (TMK, IWK and CHS). Only one station (CHS) is common to two data sets. From this inversion, we can become clear three results. (1) Qs-value of crust obtained by the inversion as a function of frequency is good agreement with those obtained by other workers with different methods. (2) Local site effects by the inversion agree well with the theoretical site amplifications by Haskell's method. (3) Source spectra by the inversion fit to the characteristics of ω^{-2} model in magnitude range M=3.9-7.0. The relation of seismic moment and corner frequency is different at the earthquake regions.

1 INTRODUCTION

Many statistical analysis of strong motion spectra have been carried out by many workers throughout the world. Most of them were based on the multiple regression models in which the characteristics of the strong ground motion is assumed to vary lineary or logarithmic lineary according to the explanatory variables such as magnitude and epicentral distance, etc. On the other hand, several authors (Papageogiou and Aki, 1983; Andrews, 1982) have tried to analyze observed seismograms to separate source and path effects. In this method, major controlling factors observed seismograms have clearly physical meaning. Iwata and Irikura (1988) have extended Andrews' method to consider both S-wave attenuation throughout propagation path and the local site effects at each station. Many workers have analyzed source, path and site effects. Source spectral models such as the ω^{-2} model (Aki, 1967), multi-crack model (Papageogiou and Aki, 1983) were used to classify the source spectra obtained from the observed seismograms. Anelasticity of the crust (Qs-value) have been

SMiRT 11 Transactions Vol. K (August 1991) Tokyo, Japan, © 1991

studied by the single station method with S-coda wave (Sato and Matsumura, 1980; Aki, 1980; Tsujiura, 1978). Local site amplification effects have been studied by multi-reflection method (Haskell's matrix method).

2 METHOD

We used the formulation of the inversion by Iwata and Irikura (1988). Spectral characteristics of observed S-wave motion at j-th site by i-th earthquake are considered to consist of three major controlling factors of source spectra, propagation path effects of attenuation by geometical spreading and by damping characteristics and local site amplification effects as follows,

$$O_{ij}(f) = S_i(f) \cdot (1/R_{ij}) \cdot \exp(-\pi f R_{ij}/Q_s(f) V_s) \cdot G_j(f) \quad (1)$$

where $O_{ij}(f)$, observed S-wave spectra at j-th site by i-th earthquake; $S_i(f)$, seismic source spectra of i-th earthquake; $Q_s(f)$, quality factor of the crust along path; V_s , average shear wave velocity along path. In order to obtain linear equations, Eq. (1) is modified by taking the logarithm;

$$\log O'_{ij}(f) = -\log R_{ref} + \log S_i(f) - (\log e) \pi f R_{ij}/Q_s(f) V_s + \log G_j(f) \quad (2)$$

where $O'_{ij}(f) = (R_{ij}/R_{ref}) O_{ij}(f)$ and R_{ref} is the arbitrary normalized distance. If seismic motions and there spectra were observed J stations by I earthquakes, we can construct $I \times J$ simultaneous equations. We shall determine at each frequency unknown values as follows,

$$I \text{ (source spectra)} + J \text{ (local site amplifications)} + 1 \text{ (} Q_s\text{-value)}$$

Because this simultaneous equations have $I \times J$ equations and $I+J+1$ unknown values, we solved resulting linear least squares problem with inequality constrains where $G_j(f) \geq 1.0$ using the singular value decomposition method (Lawson and Hanson, 1974).

3 DATA SETS

Accelerograms have been recorded by seismic net work array stations in Kanto District operated Strong Ground Observing Project of the Association of Electric Power Companies in Japan. Among the earthquake records from 1979/6 to 1983/6, we used two independent data sets according to two different regions. Fig. 1 shows the hypocentral locations by JMA and the stations used in our study. Symbol (o) in Fig. 1 are for earthquakes occurred in the southern part of Kanto District with $M=5.7-7.0$ recorded at four stations; SZJ (Shuzenji), TTY (Tateyama), HMY (Higashimatsuyama), CHS (Chyoshi) (data set-1), the other symbol (Δ) are in the northern part with $M=5.6-6.6$ recorded at three stations; TMK (Tomioka), IWK (Iwaki) and CHS (Chyoshi) (data set-2). Only CHS is common to two data set of 1, 2. Strong motion accelerometers of SZJ, TTY and HMY were installed at G.L.-100m and in the rock S-wave velocity $V_s=0.7-0.8$ km/sec, CHS at G.L.-18m in the rock $V_s=1.4$ km/sec, TMK and IWK at G.L.-950m and -330m in the rock $V_s=2.8$ km/sec.

The procedure of obtaining Fourier amplitude spectra in data set of 1, 2 is as follows. We analyzed the S-wave portion of the two horizontal components (NS and EW components). The S-wave portion is defined Dobry, Idriss and Ng (1978). Thus, from observed accelerations of two horizontal components, we took filter (high pass filter of frequency ≥ 5.0 Hz) and calculated arias intensity I_0 and root mean square r.m.s. of acceleration. Fig. 2 shows the relation of I_0 , r.m.s. and time. We divided the time from $I_0=2\%$ to 95% by the least squares method (Anderberg, 1973). The S-wave portion is the part of max. r.m.s. acceleration or the part of max. inclination of I_0 . We analyzed the S-wave portion and calculated Fourier amplitude spectra. Fourier spectra $O_{ij}(f)$ for the inversion were obtained by the vectorial summation of the horizontal components.

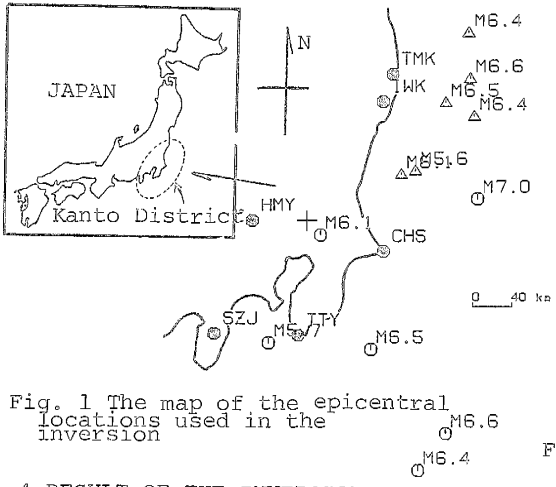


Fig. 1 The map of the epicentral locations used in the inversion

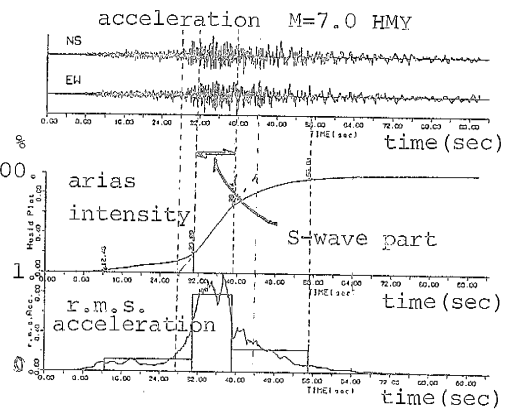


Fig. 2 An example of acceleration seismograms and these arias intensity I and r.m.s. acceleration

4 RESULT OF THE INVERSION

4.1 Q_s -value as a function of frequency

Fig. 3 (a) shows the $1/Q_s(f)$ obtained by the inversion as a function of frequency using data set 1 of the southern part of Kanto District. Fig. 3 (b) shows the result using data set 2 of northern part. Both results of $1/Q_s(f)$ clearly tend to decrease with frequency and have nearly same value than 1.0Hz. The frequency dependence of Q_s -value is roughly proportional to (frequency) $^{0.78}$ than 1.0Hz (thus, $Q_s=100f^{0.78}$) In Fig. 3, we also plotted relations of $1/Q_s$ -value and frequency obtained by other method. The results are good agreement with the results of Aki (1979), Tsujiura (1978) in Kanto District. It is interesting that the relation of $1/Q_s(f)$ and frequency shows extreme values at low frequency domain and this result have been suggested by Aki (1979). The frequency of this extreme value may have important meaning. Assuming the crust is random medium, this frequency corresponds to the characteristic crack length (Yamashita,1990, Matsunami,1990).

4.2 Local site effects

Fig. 4 (a) shows the local site effects obtained from data set 1 and (b) shows the result obtained from data set 2. The site amplification of CHS station in data set 1, 2 must be the same in Fig. 4. Putting local site effect of TMK is equal 1.0, the other site amplification effects are shown in Fig. 5. Table 1 shows the structure parameters (SZJ, TTY, HMY and CHS) for the theoretical calculation using Haskell's method including the effects of inelastic attenuations. The results of theoretical calculation are shown in Fig. 5. The site effects by the inversion agree well with the theoretical site amplification factors.

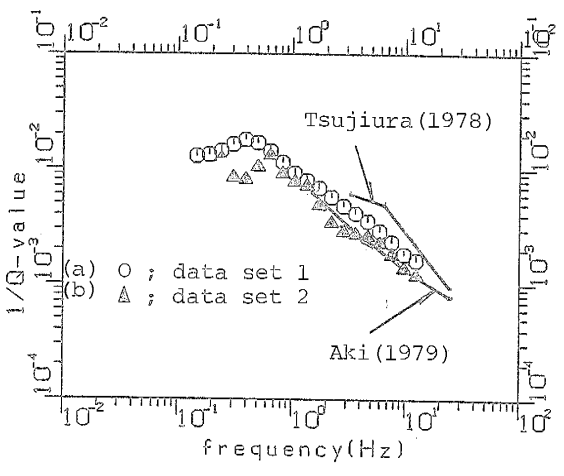


Fig. 3 Q_s -value by the inversion as a function of frequency.

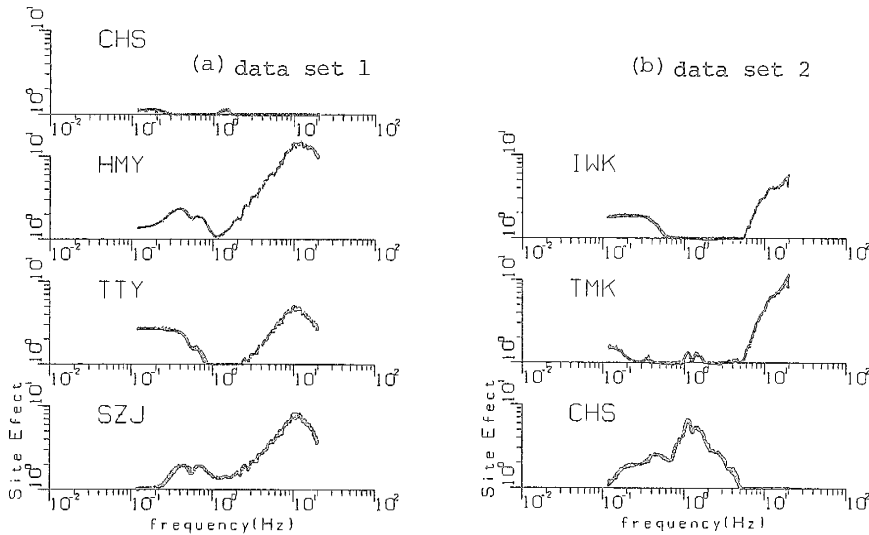


Fig. 4 The site amplification effects by the inversion.

Table 1 structure parameters

| SZJ(Syuzenji) | | | | TTY(Tateyama) | | | |
|---------------|---------|-------|-------|---------------|---------|-------|-------|
| 1) | 2) | 3) | 4) | 1) | 2) | 3) | 4) |
| 1 | 1.4 | 350. | 0.047 | 1 | 3.0 | 100. | 0.080 |
| 2 | 5.6 | 200. | 0.032 | 2 | 4.0 | 280. | 0.021 |
| 3 | 4.6 | 300. | 0.019 | 3 | 6.9 | 400. | 0.013 |
| 4 | 6.9 | 690. | 0.006 | 4 | 5.9 | 560. | 0.008 |
| 5 | 3.9 | 220. | 0.029 | 5 | 6.1 | 280. | 0.021 |
| 6 | 7.3 | 500. | 0.010 | 6 | 42.1 | 600. | 0.008 |
| 7 | 3.9 | 160. | 0.043 | 7 | 34.0 | 640. | 0.007 |
| 8 | 7.3 | 650. | 0.007 | 8 | 198.0 | 640. | 0.007 |
| 9 | 4.4 | 280. | 0.021 | 9 | 2000.0 | 1500. | 0.002 |
| 10 | 6.7 | 850. | 0.005 | 10 | 5000.0 | 2500. | 0.001 |
| 11 | 5.6 | 330. | 0.017 | 11 | 6200.0 | 3100. | 0.001 |
| 12 | 3.4 | 690. | 0.006 | 12 | 14000.0 | 3900. | 0.001 |
| 13 | 2.0 | 400. | 0.013 | | | | |
| 14 | 10.0 | 650. | 0.007 | | | | |
| 15 | 2.1 | 350. | 0.016 | | | | |
| 16 | 6.0 | 650. | 0.007 | | | | |
| 17 | 4.0 | 850. | 0.005 | | | | |
| 18 | 4.6 | 600. | 0.008 | | | | |
| 19 | 5.4 | 800. | 0.005 | | | | |
| 20 | 4.9 | 700. | 0.006 | | | | |
| 21 | 200.0 | 700. | 0.006 | | | | |
| 22 | 700.0 | 1450. | 0.002 | | | | |
| 23 | 1000.0 | 2300. | 0.001 | | | | |
| 24 | 2000.0 | 2500. | 0.001 | | | | |
| 25 | 15000.0 | 3700. | 0.001 | | | | |
| 26 | 17000.0 | 3900. | 0.001 | | | | |

- 1) layer No.
 2) thickness H(m)
 3) S-wave velocity Vs (m/sec)
 4) damping h
 $h=1/2Q$

| HMY(Higashimatsuyama) | | | | CHS(Chyoshi) | | | |
|-----------------------|---------|-------|-------|--------------|---------|-------|-------|
| 1) | 2) | 3) | 4) | 1) | 2) | 3) | 4) |
| 1 | 1.9 | 300. | 0.019 | 1 | 1.3 | 110. | 0.070 |
| 2 | 10.6 | 650. | 0.007 | 2 | 2.9 | 220. | 0.029 |
| 3 | 9.7 | 1000. | 0.004 | 3 | 2.0 | 330. | 0.017 |
| 4 | 13.8 | 700. | 0.006 | 4 | 2.2 | 540. | 0.009 |
| 5 | 10.7 | 900. | 0.005 | 5 | 0.9 | 450. | 0.011 |
| 6 | 4.1 | 450. | 0.011 | 6 | 2.9 | 1020. | 0.004 |
| 7 | 27.6 | 750. | 0.006 | 7 | 1.3 | 700. | 0.005 |
| 8 | 5.9 | 600. | 0.008 | 8 | 1.9 | 1050. | 0.004 |
| 9 | 14.4 | 750. | 0.006 | 9 | 2.6 | 1400. | 0.003 |
| 10 | 5.9 | 650. | 0.007 | 10 | 282.0 | 1400. | 0.003 |
| 11 | 14.5 | 750. | 0.006 | 11 | 100.0 | 2500. | 0.001 |
| 12 | 179.0 | 750. | 0.006 | 12 | 4500.0 | 3100. | 0.001 |
| 13 | 1000.0 | 1500. | 0.002 | 13 | 10600.0 | 3400. | 0.001 |
| 14 | 4500.0 | 3000. | 0.001 | 14 | 16900.0 | 3700. | 0.001 |
| 15 | 10600.0 | 3400. | 0.001 | | | | |
| 16 | 16900.0 | 3700. | 0.001 | | | | |

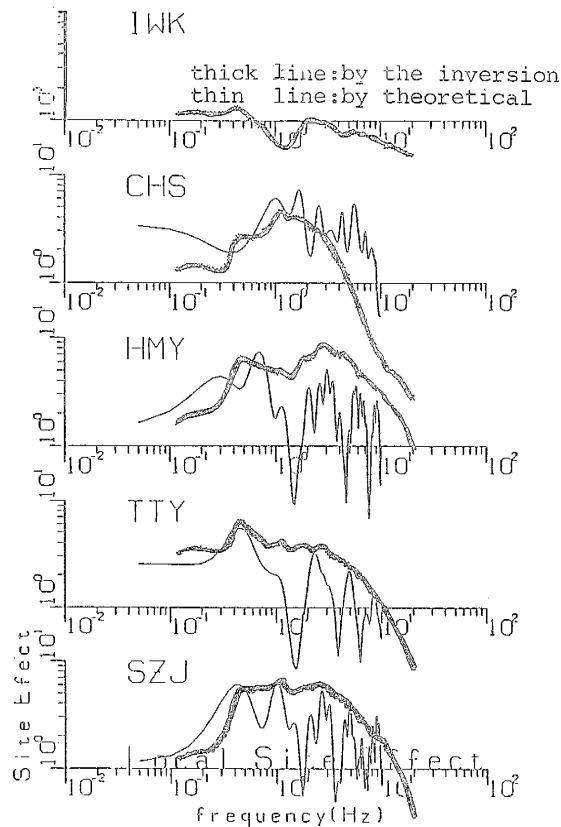


Fig. 5 The site amplification effects determined by the inversion and the result by theoretical method.

4.3 Source spectra

Source displacement spectra obtained by the inversion are plotted in Fig. 6 (a) data set 1, (b) data set 2, putting local site effect of TMK equal 1.0. In Fig. 6, we showed corner frequency f_0 by using Andrews(1986) method. Source displacement spectra have flat level at low frequency and have f_0 and tend to decrease with frequency, being proportional to (frequency) $^{-2}$. These results show that source displacement spectra fit to ω^{-2} model.

In the inversion, we can get propagation path effect, $\exp(-\pi f R_{ij}/Q_s V_s)/R_{ij}$ and local site amplification effects, $G_j(f)$ at each site. Then we shall determine source spectra using the earthquake records from 1979/6 to 1963/6 by the equation as follows,

$$S_i(f) = [R_{ij} \cdot \exp(-\pi f R_{ij}/Q_s V_s) / G_j(f)] \cdot O_{ij}(f) \quad (3)$$

Fig. 7 shows the hypocentral locations by JMA from 1979/6 to 1983/6. We plotted hypocentral location by alphabet symbols at each earthquake region. Then we determined source spectra using Eq. (3). Specially we determined seismic moment as follows,

$$M_0 = 4\pi \rho V_s^3 r / R\phi \Omega_0$$

where ρ ; density = 2.7g/cm³, r ; hypocentral distance, $R\phi$; radiation pattern = 0.63, V_s ; shear wave velocity = 3.7km/sec, Ω_0 ; the flat level of source displacement spectra at low frequency. On the other hand, we determined corner frequency by Andrews' method. Fig. 8 shows the relation M_0 and corner frequency f_0 at each earthquake region (see Fig. 7). Seismic moment M_0 is proportional to (corner frequency) $^{-3}$ with some band width. We can say that M_0 - f_0 relation is different according to the earthquake regions, roughly divided into northern part (K, H and I regions) and southern part (B, L and N regions) in Kanto District. Then we shall conclude that source displacement spectra fit to ω^{-2} model in magnitude range 3.9-7.0 and differ for each region.

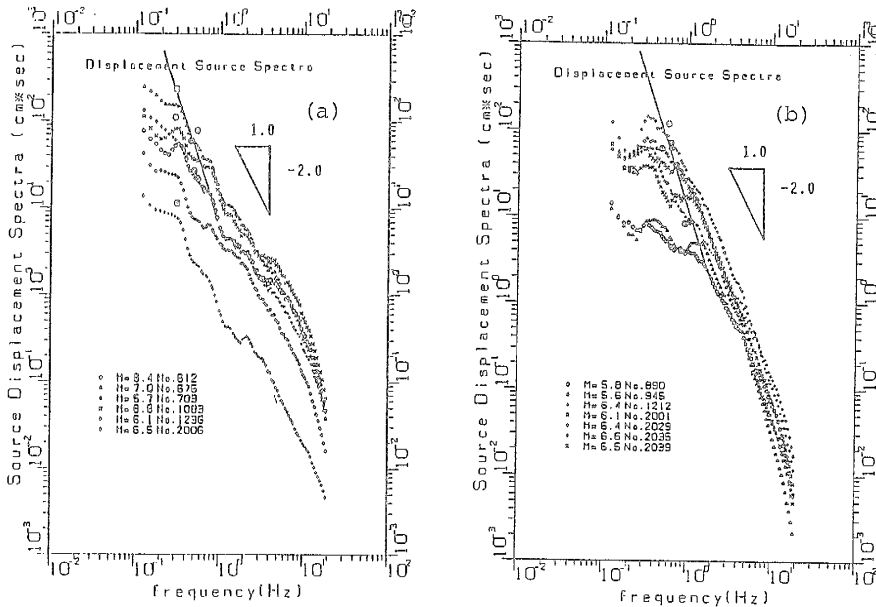


Fig. 6 The source displacement amplitude spectra determined by the inversion.

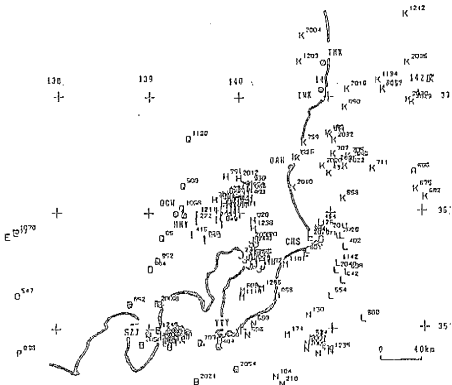


Fig. 7 The map of the epicentral locations
5 CONCLUSION (1979-1983)

In recent years, earthquake records were observed by seismic net work array system at many regions. Our inversion method based upon multi-array data in a local region is very efficient to evaluate source effects, propagation path effects and local site effects using earthquake records of these seismic array system. The three major controlling factors separated by this inversion are good agreement with the results of the workers by different theoretical methods. We predict the strong ground motion at the site, we must consider local path effect and characteristic local scaling law (local relation of seismic moment M_0 and corner frequency f_0 , or seismic moment M_0 and fault area $S = \pi r^2$, $r = 0.28X V_s/f_0$). Then we can predict strong ground motion summing small events recorded at the site with ω^{-2} scaling law (Irikura, 1983)

ACKNOWLEDEMENT: The seismic records used in this paper were obtained by the joint research study on electric power companies in Japan, entitled "Study on the characteristics of seismic wave".

REFERENCES

Andrews, D.J. (1982): Separation of source and propagation spectra of seven Mammoth Lakes aftershocks, Proceedings of Workshop, Dynamic characteristics of faulting, U.S. Geol. Sur., Open File Rep., 437.
 Iwata, T. and Irikura, K. (1988): Source parameters of the 1983 Japan Sea Earthquake Sequence, J. Phys. Earth, 36.
 Aki, K. (1967): Scaling relation of seismic spectrum, J. Geophys. Res., 72.
 Papageorgiou, A.S. and Aki, K. (1983): A specific barrier model for the quantitative description of inhomogeneous faulting and the prediction of strong ground motion, Bull. Seis. Soc. Am., 73.
 Sato, H. and Matsumura, S. (1980): Three dimensional analysis of scattered P waves on the basis of the PP single isotropic scattering model, J. Phys. Earth, 28.
 Aki, K. (1980): Attenuation of shear waves in the lithosphere for frequencies from 0.05 to 25 Hz, Phys. Earth Planet, 21.
 Tsujiura, M. (1978): Spectral analysis of the coda waves from local earthquakes, Bull. Earthquake Res. Inst., Univ. Tokyo, 21.
 Lawson, C.L. and Hanson, R.J. (1974): Solving least squares problem, Prentice-Hall.
 Dobry, R., Idriss, I.M. and Ng, E. (1978): Duration characteristics of horizontal components of strong-motion earthquake record, Bull. Seis. Soc. Am., 68.
 Anderberg, M.R. (1973): Cluster analysis for applications, Academic Press, Inc.
 Yamashita, T. (1990): Attenuation and dispersion of SH waves due to scattering by randomly distributed cracks, PAGEOPH, 132, No. 3.
 Matsunami, K. (1990): Laboratory measurements of spatial fluctuation and attenuation of elastic waves by scattering due to random heterogeneities, PAGEOPH.
 Andrews, D.J. (1986): Objective determination of source parameters and similarity of earthquakes of different size, in Earthquake Source Mechanics, Maurice Ewing Series 6.

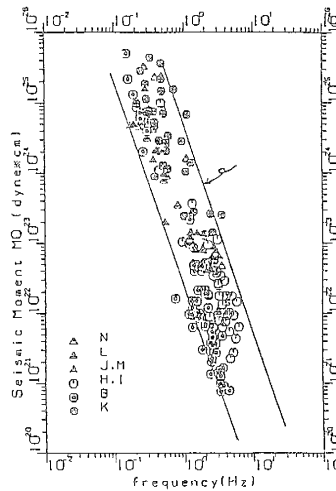


Fig. 8 The logarithm of M_0 versus the logarithm of f_0 .